of the crystalline conformations and LD3 appear relative large (i.e., approximately 60°), it is evident that all five conformations reside within a broad shallow potential energy well. Quantitatively, these conformations in the crystal would be expected to differ from LD3 by less than 3 kcal/mol. In effect, this work supports the notion that for aspartyl-based taste ligands conformations in solution and in the crystal are closely related to each other.

## Conclusions

For the sweet L,D stereoisomer (alitame) the minimum energy conformation supported most strongly by the experimental and theoretical data taken together is LD3. On the basis of our existing model, this conformer would be predicted to be sweet. For the bitter L,L stereoisomer of alitame, the conformations that clearly fit the NMR data best are LL5, LL7, and LL8. All three of these conformers would be predicted to be bitter. For the tasteless D,D stereoisomer of alitame, the conformations that clearly fit the NMR data best are the mirror images of LL5, LL7, and LL8. All three of these conformers would be predicted to be tasteless. Each of these minimum energy conformations can be considered a "snapshot" of the preferred conformations of the species in solution. Given the flexibility and kinetic energy of molecules in solution it is best to consider all of the above conformers as contributing species in a dynamic structure. Our model correctly predicts the taste properties of each stereoisomer's contributing conformers. In addition, the average of the minimum energy structures for each isomer retains the conformational characteristics consistent with its observed taste, as predicted by our model.

**Acknowledgment.** The authors gratefully acknowledge a grant from the National Institute of Dental Research, DE05476. In addition, NIH Grant RR03342-01 and NSF Grant BBS86-12359 helped support our NMR facility. Our X-ray facility is supported in part by NSF instrumentation Grant CHE-8904832. The work of E. Benedetti was supported in part by Grants CNR AI.90.00133.03 and CNR AI.90.01790.14. Alitame and the stereoisomers of alitame were generously supplied by Dr. Raymond Gloacky and associates of Charles Pfizer and Co.

**Supplementary Material Available:** Tables of atomic coordinates and isotropic coefficients, bond lengths and angles, H-atom coordinates and isotropic coefficients, anisotropic coefficients, and solution and refinement data, experimental data, and a figure consisting of the alitame structure (11 pages); table of observed and calculated structure factors (19 pages). Ordering information is given on any current masthead page.

# A New Photolysis Intermediate in Artificial and Native Visual Pigments

**C. E. Randall,[1a,d] J. W. Lewis,[1a] S. J. Hug,[1a] S. C. Björling,[1a] I. Eisner-Shanas,[1b] N. Friedman,[1b] M. Ottolenghi,[1c] M. Sheves,*[,1b] and D. S. Kliger*[,1a]**

*Contribution from the Department of Chemistry, University of California, Santa Cruz, Santa Cruz, California 95064, Department of Organic Chemistry, Weizmann Institute of Science, Rehovot 76 100, Israel, and Department of Physical Chemistry, The Hebrew University of Jerusalem, Jerusalem 91 904, Israel.* *Received August 13, 1990. Revised Manuscript Received December 31, 1990*

**Abstract:** Nanosecond time-resolved and continuous illumination, low-temperature, spectroscopic studies reveal a new photolysis intermediate in a wide variety of artificial visual pigments as well as in native rhodopsin. This new intermediate, BSI, has a blue-shifted spectrum relative to the pigments as well as to their batho and lumi intermediates. At room temperature BSI is formed subsequent to batho and approaches an equilibrium with batho before decaying to the lumi intermediate. Chromophore modifications, which modify the β-ionone ring, eliminate conjugation between the ring and the polyene chain, add bulky groups to the $C_4$ position on the ring, or remove the 13-methyl group all yield time-resolved spectra which lead to the general scheme

$$\text{rho} \xrightarrow{h\nu} \text{batho} \rightleftarrows \text{BSI} \rightarrow \text{lumi...}$$

The same mechanism is shown to be valid in isorhodopsin and in the native bovine pigment rhodopsin. Chromophore modifications described above affect the batho ⇄ BSI equilibrium as well as the kinetics of approach to equilibrium but have little effect on the spectra of the intermediates or on the rate of the BSI to lumi transition. Implications for the nature of the BSI intermediate are discussed. Though BSI has a spectrum blue-shifted from that of batho, BSI is higher in enthalpy. It is proposed that this apparent conflict may be due to the fact that the photon energy, initially stored in chromophore–protein interactions, is transmitted to the protein during the batho-to-BSI transition. If energy at the BSI stage is still stored in the chromophore, models simply relating energy storage to bathochromic shifts must be ruled out.

## Introduction

The complex series of reactions leading to visual transduction in vertebrates is initiated by light absorption of the visual pigment rhodopsin (rho). Rho consists of an 11-*cis*-retinal chromophore (Figure 1, I) bound via a protonated Schiff's base to the ε-amino group of lysine 296 in the protein opsin. It is now widely accepted that bathorhodopsin (batho-rho), the first photointermediate which can be trapped at low (liquid nitrogen) temperatures, results from a cis to trans photoisomerization of the 11,12-double bond.[2-10]

(1) (a) University of California, Santa Cruz. (b) Weizmann Institute of Science. (c) The Hebrew University of Jerusalem. (d) Currently at The Laboratory for Atmospheric and Space Physics, University of Colorado, Boulder, CO.

(2) Hubbard, R.; Kropf, A. *Proc. Natl. Acad. Sci. U.S.A.* **1958**, *44*, 130-139.
(3) Rosenfeld, T.; Honig, B.; Ottolenghi, M.; Hurley, J.; Ebrey, T. G. *Pure Appl. Chem.* **1977**, *49*, 341-351.
(4) Honig, B. *Annu. Rev. Phys. Chem.* **1978**, *29*, 31-57.
(5) Akita, H.; Tanis, S. P.; Adams, M.; Balogh-Nair, V.; Nakanishi, K. *J. Am. Chem. Soc.* **1980**, *102*, 6370-6372.
(6) Ottolenghi, M. *Adv. Photochem.* **1980**, *12*, 97-200.

0002-7863/91/1513-3473$02.50/0 

Transient absorbance changes on picosecond time scales, either at low temperatures[11] or room temperature,[12,13] have been attributed to a red-shifted precursor of batho-rho, denoted as prebatho-rho[14] and photo-rho, respectively. The specific conformation of the chromophore in batho-rho is not well understood. Various electrostatic interactions between the chromophore and the protein as well as conformational distortions in the chromophore have been suggested as causes for batho-rho's red-shifted spectrum and for its ability to store ~32 kcal/mol of the photon energy absorbed by rho.[15-21] Even more ambiguous is the nature of photo-rho (see reviewing discussion in ref 22). In any event, it is well-established that a cis-to-trans isomerization of the chromophore occurs only in the presence of light and that this is a primary result of light absorption by rho.

At liquid nitrogen temperatures, irradiation of rho results in a photoequilibrium between rho ($\lambda_{max}$ = 498 nm), batho-rho ($\lambda_{max}$ = 543 nm), and isorhodopsin (iso, with a 9-*cis*-retinal chromophore, Figure 1, II, $\lambda_{max}$ = 483 nm) produced by photolysis of batho-rho. Upon warming above −140 °C, batho-rho is converted to lumirhodopsin (lumi-rho, $\lambda_{max}$ = 497 nm). Lumi-rho decays to metarhodopsin I (meta-I-rho, $\lambda_{max}$ = 478 nm) at temperatures higher than −40 °C, which then decays to metarhodopsin II (meta-II-rho, $\lambda_{max}$ = 380 nm) at temperatures higher than −15 °C. Under physiological conditions the meta-II-rho intermediate is assumed to be responsible for eventual activation of an enzyme cascade, leading to closing of sodium channels in the plasma membrane and neuronal transmission of the visual signal. Clearly, it is of interest to study the nature of each of these photointermediates in order to understand the mechanism by which the transduction process is triggered.

Until relatively recently, it was widely believed that at room temperature batho-rho decays on the time scale of $10^{-7}$ s to lumi-rho, followed by a decay of lumi-rho to meta-I-rho in about 20 μs. However, there has been substantial evidence in the past several years that the steps preceding meta-I-rho, after the formation of batho-rho, are more complicated than a sequence of simple unidirectional steps as previously thought. In fact, as early as 1962 Grellman et al. proposed the existence of multiple forms of batho-rho.[23] Later Applebury suggested the possibility of an equilibrium between lumi-rho and meta-I-rho.[24] In a series of papers on low-temperature spectroscopy of both frog and bovine rhodopsin, Yoshizawa and co-workers claimed the existence of two forms of batho-rho.[25-27] We subsequently investigated the room-temperature photolysis of bovine rho[28] and found kinetic and spectral behavior on the nanosecond time scale which seemed consistent with the findings of Sasaki et al. We thus proposed that two forms of batho-rho were also formed at room temperature and decayed in parallel to either one or two lumi-rho products.

Experiments with artificial rhodopsins, based on the exchange of the native 11-*cis*-retinal chromophore with a suitably tailored

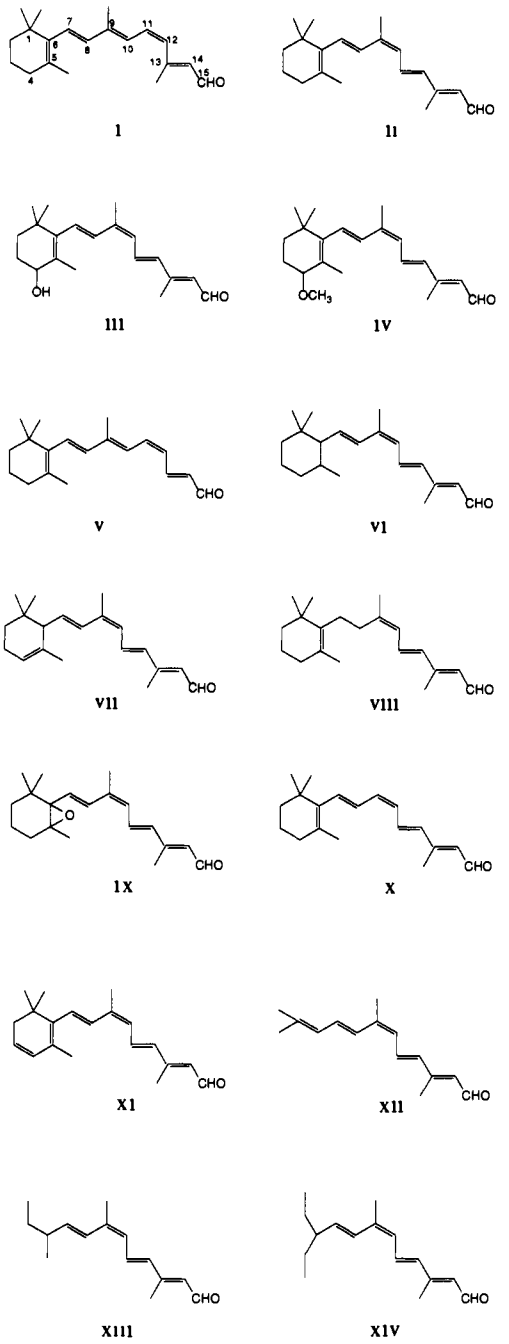


**Figure 1.** Synthetic retinal analogues used for preparing artificial visual pigments: (I) native rhodopsin, (II) isorhodopsin, (III) 4-hydroxyisorhodopsin, (IV) 4-methoxyisorhodopsin, (V) 13-desmethylrhodopsin, (VI) 5,6-dihydroisorhodopsin, (VII) α-isorhodopsin, (VIII) 7,8-dihydroisorhodopsin, (IX) 5,6-epoxyisorhodopsin, (X) 9-desmethylisorhodopsin, (XI) 3,4-dehydroisorhodopsin, (XII) acyclic isorhodopsin XII, (XIII) acyclic isorhodopsin XIII, and (XIV) acyclic isorhodopsin XIV.

(7) Birge, R. R. *Annu. Rev. Biophys. Bioeng.* **1981**, *10*, 315-354. Birge, R. R. *Biochim. Biophys. Acta* **1990**, *1016*, 293-327.
(8) Mao, B.; Tsuda, M.; Ebrey, T. G.; Akita, H.; Balogh-Nair, V.; Nakanishi, K. *Biophys. J.* **1981**, *35*, 543-546.
(9) Packer, L. *Methods, Enzymol., Biomembranes, Part I* **1982**, 81.
(10) Fukada, Y.; Shichida, Y.; Yoshizawa, T.; Ito, M.; Kodama, T.; Tsukida, K. *Biochemistry* **1984**, *23*, 5826-5832.
(11) Peters, K. S.; Applebury, M. L.; Rentzepis, P. M. *Proc. Natl. Acad. Sci. U.S.A.* **1977**, *74*, 3119-3123.
(12) Shichida, Y.; Matuoka, S.; Yoshizawa, T. *Photobiochem. Photobiophys.* **1984**, *7*, 221-228.
(13) Shichida, Y. *Photobiochem. Photobiophys.* **1986**, *13*, 287-307.
(14) Dinur, U.; Honig, B.; Ottolenghi, M. *Photochem. Photobiol.* **1981**, *33*, 523-527.
(15) Honig, B.; Dinur, U.; Nakanishi, K.; Balogh-Nair, V.; Gawinowicz, M. A.; Arnaboldi, M.; Motto, M. G. *J. Am. Chem. Soc.* **1979**, *101*, 7084-7086.
(16) Honig, B.; Ebrey, T.; Callender, R. H.; Dinur, U.; Ottolenghi, M. *Proc. Natl. Acad. Sci. U.S.A.* **1979**, *76*, 2503-2507.
(17) Birge, R. R.; Hubbard, L. M. *J. Am. Chem. Soc.* **1980**, *102*, 2195-2205.
(18) Warshel, A.; Barboy, N. *J. Am. Chem. Soc.* **1982**, *104*, 1469-1476.
(19) Ottolenghi, M.; Sheves, M. In *Primary Processes in Photobiology*; Kobayashi, T., Ed.; **1987**; pp 144-153.
(20) Palings, I.; Pardoen, J. A.; van den Berg, E.; Winkel, C.; Lugtenburg, J.; Mathies, R. A. *Biochemistry* **1987**, *26*, 2544-2556.
(21) Birge, R. R.; Einterz, C. M.; Knapp, H. M.; Murray, L. P. *Biophys. J.* **1988**, *53*, 367-385.
(22) Ottolenghi, M.; Sheves, M. *J. Mem. Biol.* **1989**, *112*, 193.
(23) Grellman, K. H.; Livingston, R.; Pratt, D. *Nature (London)* **1962**, *193*, 1258-1260.
(24) Applebury, M. L. *Vision Res.* **1984**, *24*, 1445-1454.
(25) Sasaki, N.; Tokunaga, F.; Yoshizawa, T. *FEBS Lett.* **1980**, *114*, 1-3.
(26) Sasaki, N.; Tokunaga, F.; Yoshizawa, T. *Photochem. Photobiol.* **1980**, *32*, 433-441.
(27) Sasaki, N.; Tokunaga, F.; Yoshizawa, T. *Biochim. Biophys. Acta* **1983**, *722*, 80-87.
(28) Einterz, C. M.; Lewis, J. W.; Kliger, D. S. *Proc. Natl. Acad. Sci. U.S.A.* **1987**, *84*, 3699-3703.

Scheme I

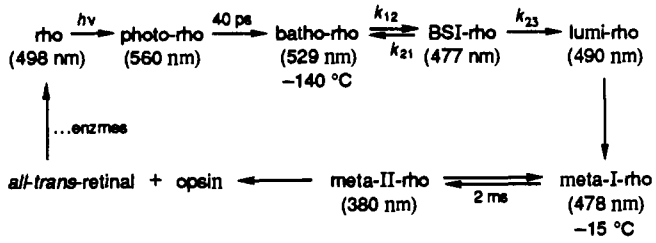


synthetic analogue (for a recent review see ref 22), led us to a revision of the two batho-rho model. The first clues were derived from the low- and room-temperature photolysis of both 13-desmethylisorhodopsin (13-dm-iso), with a 9-*cis*-13-desmethylretinal, and *cis*-5,6-dihydroisorhodopsin (5,6-diH-iso), with a *cis*-5,6-dihydro-9-*cis*-retinal chromophore (see Figure 1, VI). In the case of 13-dm-iso, early low-temperature work by Yoshizawa and co-workers suggested the existence of a blue-shifted species (denoted as BL-13-dm-iso) formed by warming batho-13-dm-iso. BL-13-dm-iso was stable over a small range of temperatures and decayed to a lumi-like product at −140 °C. This apparent anomaly in the photoreaction was also observed at room temperature for both 13-desmethylisorhodopsin and 13-desmethylrhodopsin (13-dm-rho), with an 11-*cis*-13-desmethylretinal chromophore.[29] Spectra observed a few nanoseconds after excitation showed little bathochromic absorbance reminiscent of batho-13-dm-rho. Instead a large blue-shifted absorbance appeared within nanoseconds of photolysis. Similar behavior was encountered in the case of 5,6-diH-iso.[30] It was concluded that in both synthetic pigments a new blue-shifted intermediate (denoted as BSI) existed between the batho and lumi stages, although its formation was not kinetically resolved. In the case of 5,6-diH-iso, this picture revised the early assignment of Yoshizawa et al. which, based on low-temperature studies, identified BSI-5,6-diH-iso as hypsorhodopsin.[31]

The above findings with artificial rhodopsins led us to reinvestigate the photolysis intermediates of native rhodopsin by measuring the temperature dependence, excitation wavelength, actinic power, and polarization dependence of the spectral changes from 15 to 4000 ns after photolysis. Use was made of a global exponential fitting approach in conjunction with a singular value decomposition (SVD) method to analyze the corresponding light-induced spectral changes. It was shown that the best fit to these and to the previously published experiments included a sequential, rather than parallel (two batho-rho), decay process.[32] The mechanism involves a single batho-rho photoproduct which approaches an equilibrium with a new, blue-shifted intermediate, BSI-rho, analogous to the BSI species observed with the above artificial pigments. Unlike the unresolvable (subnanosecond) equilibration in the artificial systems, equilibration in native rho occurs on an ~36-ns time scale. Because of the relative values of the rate constants for the formation and decay of BSI-rho and the formation of lumi-rho (from the batho-rho/BSI-rho mixture), a true equilibrium is never reached; i.e., lumi-rho forms before BSI-rho and batho-rho reach steady-state concentrations. By using the rate constants, however, we calculated a batho-rho ⇄ BSI-rho equilibrium constant at room temperature of about 1.4. In summary, we believe the following mechanism best describes the thermal processes which occur on a nanosecond time scale after photolysis of rho.

At both low temperature and room temperature, the existence of BSI in the pigment analogues mentioned above was readily apparent from the absorption spectrum at a particular temperature and time after photolysis. In the case of native rhodopsin, the presence of such a blue-shifted product at early times (nanoseconds) after photolysis is not obvious. However, as previously described,[32] when a global exponential analysis is performed, it becomes clear that Scheme I is the most suitable mechanism to explain the room-temperature transduction process of native rho as well.

In the present paper we examine a large variety of artificial rhodopsins and show that the appearance of the BSI intermediate is a common characteristic of many modified chromophores. We also demonstrate that the pigment analogue results are consistent with the physiologically relevant mechanism in rho itself. The analysis includes data which has already been reported in the literature for rho (I),[32] 13-dm-rho (V),[29] iso (II),[33] and 5,6-diH-iso (VI).[30] In addition, we present a new analysis of the iso and 5,6-diH-iso data by using the global fitting and SVD methods. We also report new results from the following visual pigment analogues: 3,4-dehydroisorhodopsin (XI, 3,4-deH-iso), α-isorhodopsin (i.e., 4,5-dehydro-5,6-dihydroisorhodopsin, α-iso, VII), 7,8-dihydroisorhodopsin (VIII, 7,8-diH-iso), 4-hydroxyisorhodopsin (III, 4-hyd-iso), 4-methoxyisorhodopsin (IV, 4-met-iso), 5,6-epoxyisorhodopsin (IX, 5,6-epox-iso), 9-desmethylisorhodopsin (X, 9-dm-iso), the acyclic isorhodopsin pigment acyclic XII (XII), and the related acyclic XIII (XIII) and acyclic XIV (XIV) pigments. The chromophore structures (referred to by Roman numerals) of all of these pigments (referred to by name or abbreviation given above) are drawn in Figure 1. The artificial pigments fall into four major classes: (a) pigments with chromophores in which the ring-chain conjugation is eliminated by double bond saturation (chromophores VI, VII, VIII, and IX), (b) pigments with substituents at the $C_4$ ring position (III and IV), (c) pigments in which the ring has been replaced by a short chain segment (XII, XIII, and XIV), and (d) pigments demethylated along the polyene chain (V and X).

## Experimental Section

The synthetic retinal analogues were prepared by using previously described methods. Synthesis of VI was carried out as previously described for the all-trans isomer.[34a] VII was prepared from α-ionone;[34b] III and XI were prepared from 4-hydroxy-β-ionone and 3,4-deH-β-ionone,[35] respectively. IV was prepared from 4-methoxy-β-ionone.[36a] VIII,[34b] IX,[37] the acyclic retinals XII, XIII, and XIV,[36b] and X[38] were prepared according to known methods.

The regeneration of the synthetic pigments from bovine opsin followed procedures previously described.[30] Spectra of all pigments contained a contribution due to *all-trans*-retinal oxime peaking at 360 nm and also a contribution due to any excess chromophore added during regeneration. The latter peaked at wavelengths ≤330 nm since the excess chromophore was converted to the alcohol form by the endogenous retinol dehydrogenase during incubation with NADPH.[30] Neither of these absorbances were significant for irradiation experiments using visible wavelengths as conducted here. Room-temperature optical measurements were performed on octyl glucoside detergent suspensions of the pigments with an optical multichannel analyzer-based laser photolysis apparatus.[39] Excitation was performed with an ~7 ns pulse of 477-nm light from a Nd:YAG-pumped dye laser for most pigments, 416-nm light (Raman shifted Nd:YAG third harmonic) for 7,8-diH-iso, 440 nm for 9-dm-iso, 5,6-epox-iso, the 4-substituted, and acyclic pigments and 532 nm (Nd:YAG second harmonic) in the case of the iso data.

For low-temperature measurements detergent suspensions of the pigments were mixed with glycerol, yielding a final 66% concentration of

(29) Einterz, C. M.; Hug, S. J.; Lewis, J. W.; Kliger, D. S. *Biochemistry* **1990**, *29*, 1485–1491.
(30) Albeck, A.; Friedman, N.; Ottolenghi, M.; Sheves, M.; Einterz, C. M.; Hug, S. J.; Lewis, J. W.; Kliger, D. S. *Biophys. J.* **1989**, *55*, 233–241.
(31) Yoshizawa, T.; Shichida, Y.; Matuoka, S. *Vision Res.* **1984**, *24*, 1455–1463.
(32) Hug, S. J.; Lewis, J. W.; Einterz, C. M.; Thorgeirsson, T. E.; Kliger, D. S. *Biochemistry* **1990**, *29*, 1475–1485.
(33) Hug, S. J.; Lewis, J. W.; Kliger, D. S. *J. Am. Chem. Soc.* **1988**, *110*, 1998–1999.
(34) (a) Spudich, J. L.; McCain, D. A.; Nakanishi, K.; Okabe, M.; Shimizu, N.; Rodman, H.; Honig, B.; Bogomolni, R. A. *Biophys. J.* **1986**, *49*, 479–483. (b) Arnaboldi, M.; Motto, M. G.; Tsujimoto, K.; Balogh-Nair, V.; Nakanishi, K. *J. Am. Chem. Soc.* **1979**, *101*, 7082–7084.
(35) Henbest, H.; Jones, E.; Owen, T. *J. Chem. Soc.* **1955**, 2765–2767.
(36) (a) Henbest, H. *J. Chem. Soc.* **1951**, 1074–1078. (b) Crouch, R.; Or, Y. *FEBS Lett.* **1983**, *158*, 139–142.
(37) Ito, M.; Kodama, A.; Murata, M.; Kobayashi, M.; Tsukida, K.; Shichida, Y.; Yoshizawa, T. *J. Nutr. Sci. Vitaminol.* **1979**, 243–245.
(38) (a) Blatz, P.; Lin, M.; Balasubramaniyan, P.; Balasubramaniyan, V.; Dewhurst, P. *J. Am. Chem. Soc.* **1969**, *91*, 5930–5931. (b) Waddel, W.; Umerua, M.; West, J. *Tetrahedron Lett.* **1978**, *35*, 3223–3226.
(39) Lewis, J. W.; Warner, J.; Einterz, C. M.; Kliger, D. S. *Rev. Sci. Instrum.* **1987**, *58*(6), 945–949.

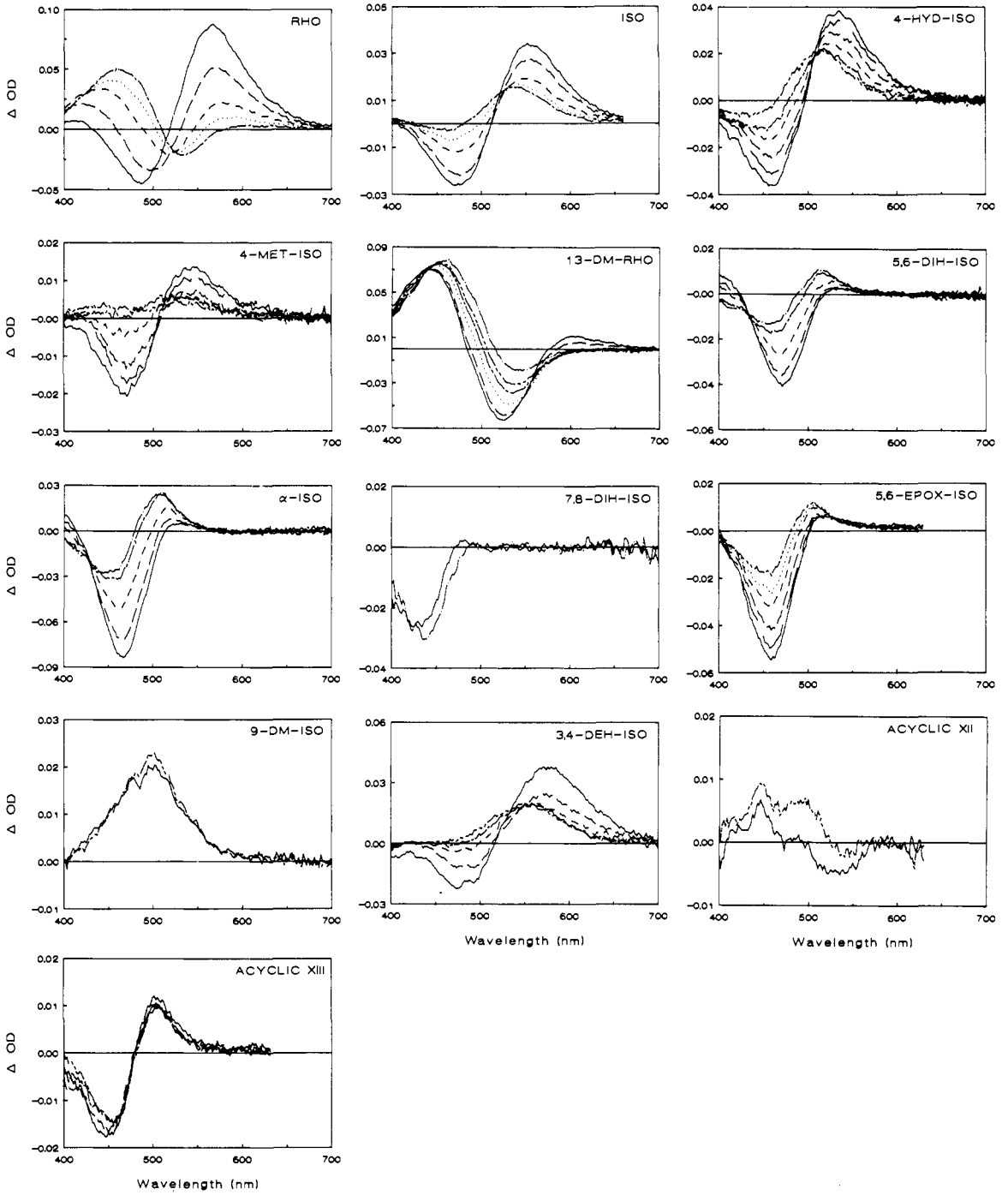


**Figure 2.** Time-dependent optical density difference spectra observed after photolysis. The times after photolysis for the curves are (—) 20 ns except for 13-dm-rho and 3,4-deH-iso where it was 15 ns and iso where it was 30 ns; (— — —) 40 ns; (- - -) 60 ns except for 5,6-epox-iso, 4-hyd-iso, 4-met-iso, and acyclic XIII where it was 80 ns; (- - -) 170 ns except for 4-hyd-iso and 4-met-iso where it was 400 ns and acyclic XIII where it was 500 ns; (···) 300 ns except for 4-hyd-iso and 4-met-iso where it was 180 ns; (- - -) 600 ns; (- - - -) 1 μs; (-·-) 4 μs except for 13-dm-rho where it was 2 μs and α-iso where it was 5 μs. Excitation was at 477 nm in all cases except for iso which was excited at 532 nm, 7,8-diH-iso which was excited at 416 nm, and 9-dm-iso, 4-hyd-iso, 4-met-iso, and acyclic XIII which were excited at 440 nm.

glycerol. The sample was cooled in a glass cryostat with quartz windows. Irradiation was carried out with a 100-W bulb with glass cutoff or interference filters for wavelength selection. Difference spectra were taken before and after irradiation. The absorption spectra were measured by a Hewlett Packard Co. (Palo Alto, CA) 8450A diode array spectrophotometer.

## Results

**(1) Room-Temperature Laser Photolysis Experiments. (a) Difference Spectra Following Laser Excitation.** All chromophores shown in Figure 1 form pigments in good yield upon incubation with bovine opsin. Artificial pigments with chromophores V–XIV have been described before. (For a review, see ref 40a and references therein. For the artificial pigment derived from retinal VII see ref 34b, and for IX and XI see ref 40b.) Difference spectra measured after photolysis of rho and the various regenerated pigments are shown in Figure 2. For most pigments a series of spectra with good signal-to-noise ratio, taken at several times from 15 to 4000 ns after photolysis, are reported. For 7,8-diH-iso, acyclic XII and acyclic XIII restrictions on quantity of pigment limited the quality of the spectra. Although noisy, it was still clear that spectra measured at intermediate times for these pigments are qualitatively consistent with the conclusions drawn below.

**I. Rho.** The difference spectra obtained for rho indicate that by 20 ns after photolysis the predominant intermediate present is a red-shifted product, batho-rho. In the 20-ns spectrum, however, the positive ΔOD in the 400–440 nm range clearly shows

the presence of an intermediate which is blue-shifted from rho itself. Even without a quantitative analysis, it is evident that these spectra do not support a simple batho-rho to lumi-rho decay. The shifting isosbestic (from about 500 nm at early times to about 525 nm at later times) is indicative of multiexponential processes. Furthermore, the later development of a reproducible isosbestic in the blue region (above 430 nm) is not consistent with the 20-ns blue absorption being merely the beginning of lumi, which is the main positive contribution in the 600-ns spectrum.

**II. Iso.** The difference spectra obtained after photolysis of iso are similar to those for rho, in that a red-shifted product which we identify as batho-iso is apparent 20 ns after photolysis. There is also a shift in the isosbestic point between spectra (although not quite as obvious as after rho photolysis), indicating that at least two processes are occurring on this time scale. Unlike rho, there is no obvious hint of a blue-shifted absorber at early times, and the 600-ns difference spectrum is significantly different from the difference spectrum measured 600 ns after photolysis of rho. Both of these points can be reconciled by the fact that the spectrum of iso, with an absorption maximum at 483 nm, is blue-shifted by 15 nm from that of rho. This tends to mask small blue absorptions such as would be expected from a BSI product (see Discussion below). Also, since the absorption maximum for lumi-rho lies near that of rho, identical lumi intermediates from rho and iso would yield a difference spectrum from iso at 600 ns after photolysis which is red-shifted from the parent pigment, as shown in Figure 2. It will be shown below that if one assumes Scheme I to be correct, the spectra of the batho, BSI, and lumi photointermediates generated from iso are remarkably similar to those observed in the photolysis of rho.

**III. 4-Hyd-iso.** The transient difference spectra observed for this artificial pigment show the increase in absorption in the red characteristic of a batho intermediate. The contribution of an early BSI species seems analogous to rho and iso and will be discussed when considering the transient spectra corrected for the bleaching of the parent pigment.

**IV. 4-Met-iso.** The transient difference spectra of 4-met-iso basically resemble those of iso and 4-hyd-iso. It is characterized, however, by a more pronounced bleaching relative to the absorption in the red at early times. Assuming similar extinction coefficients in the three systems, 4-met-iso appears to be inconsistent with the formation of a single red-shifted batho intermediate.

**V. 13-Dm-rho.** This pigment exhibits a clear example of light-induced difference spectra which look dramatically different from those acquired after photolysis of rho. While there appears to be some contribution from a red-shifted photoproduct present 15 ns after photolysis, the major feature in the 15-ns spectrum consists of a blue-shifted photoproduct. Since 13-dm-rho and rho absorb at nearly the same wavelengths, the intermediate giving rise to the positive $\Delta$OD in the blue region of the spectrum is shifted to the blue of both 13-dm-rho and rho itself. At later times the blue-shifted absorption increases and shifts slightly to the red, while the red-shifted absorption disappears. As in rho photolysis, the isosbestic point between spectra, which first appears near 540 nm, shifts to the red as time progresses, indicating multiexponential behavior.

**VI. 5,6-DiH-iso.** As in the case of 13-dm-rho the difference spectra measured after photolysis of this ring-modified pigment appear significantly different from those of rho and iso. A blue-shifted intermediate is immediately evident 20 ns after photolysis, with only a hint of a red-shifted absorber at this time. By 4000 ns, however, the difference spectrum looks similar to that seen in iso on a comparable time scale, although in 5,6-diH-iso the ratio of transient bleaching to transient absorption is larger than in iso.

**VII. $\alpha$-Iso.** This is another example of a pigment in which conjugation between the ring and polyene portions of the retinal chromophore is disrupted. The difference spectra measured after photolysis of this pigment are qualitatively the same as those measured after photolysis of 5,6-diH-iso.

**VIII. 7,8-DiH-iso.** Conjugation between the ring and the polyene chain can also be disrupted by removal of the 7,8-double bond, as in 7,8-diH-iso, a pigment which had been previously studied at low temperature.[41] In Figure 2 we show the difference spectra measured 20 and 4000 ns after photolysis of 7,8-diH-iso. Although these spectra are noisier than those of the pigments derived from VI and VII, it is evident that the predominant feature at early times in all three pigments is the large bleaching which is not accompanied by a substantial absorbance increase in the red. However, in contrast to the other pigments with disrupted conjugation, in the 7,8-diH pigment there is no increase in OD in any region of the spectra to the blue of about 470 nm. Also, at 4000 ns after photolysis, the bleaching is larger than in the 5,6-diH-iso pigments. Still, the main conclusion that can be drawn simply by inspection of the difference spectra is that, as in the 5,6-diH-iso and $\alpha$-iso pigments, no red-shifted photointermediate analogous to batho from iso or rho is apparent.

**IX. 5,6-Epox-iso.** The basic behavior of this pigment (large bleaching and small increment in the red) is analogous to the pigments from chromophores V–VIII, with details which are intermediate between VI and VII.

**X. 9-Dm-iso.** This pigment, previously studied by low-temperature FTIR spectroscopy,[42] exhibits a different class of behavior in that the room-temperature absorbance changes induced by illumination show essentially no variation on the 20 ns–1 $\mu$s time scale.

**XI. 3,4-DeH-iso.** In this pigment, instead of disrupting conjugation between the ring and polyene chain, it is extended farther into the ring. Comparison of its transient spectra with the difference spectra obtained after photolysis of iso shows that the additional double bond does little to perturb the events after photolysis.

**XII and XIII. Acyclic XII and Acyclic XIII.** Both acyclic 9-cis pigments show small and invariant absorbance changes on the 20 ns–1 $\mu$s time scale.

**(b) Corrected Difference Spectra (Time-Dependent Spectra of Intermediates).** While much information can be gained by studying the difference spectra obtained after photolysis of a pigment, this kind of analysis can also be misleading. For instance, the difference spectra obtained after photolysis of rho and iso look considerably different, yet we will show below that they are indicative of essentially identical photointermediates. The problem arises from two principal causes. One is that each parent pigment has a different wavelength of maximum absorption, so that even if identical intermediates are formed the difference spectra between the intermediates and the parent pigments will appear different. The other reason is that at high enough excitation powers, photolysis of an 11-cis pigment can result in the formation of the 9-cis analogue (by secondary photolysis which isomerizes a subsequent trans intermediate) and vice versa. While this will not contribute to a time-dependent signal (i.e., it is constant over time after the laser pulse), it can significantly alter the shapes of all spectra measured after photolysis. Moreover, difference spectra reveal little when the absorption spectrum of the intermediate is close to that of the parent pigment.

It is often preferable, therefore, to examine the actual absorption spectra at various times after photolysis, rather than the absorption difference spectra. The absorption spectra can be obtained from the difference spectra only if one knows the amount of pigment bleached and the amount of 9-cis (or 11-cis) isomer formed during the laser pulse. We have developed a procedure to measure both of these parameters, which is described in detail elsewhere.[30] Briefly, we measure a "bleaching spectrum", which consists of the difference between light transmitted through the unbleached pigment and light transmitted through a sample several seconds

(40) (a) Derguini, F.; Nakanishi, K. *Photobiochem. Photobiophys.* **1986**, *13*, 259–283. (b) Azuma, H.; Azuma, K.; Kito, Y. *Biochim. Biophys. Acta* **1973**, *295*, 520–526.

(41) Moto, O.; Tokunaga, F.; Yoshizawa, T.; Kamat, V.; Blatchly, H. A.; Balogh-Nair, V.; Nakanishi, K. *Biochim. Biophys. Acta* **1984**, *766*, 597–602.

(42) Ganter, U. M.; Schmid, E. D.; Perez-Sala, D.; Rando, R. R.; Siebert, F. *Biochemistry* **1989**, *28*, 5954–5962.

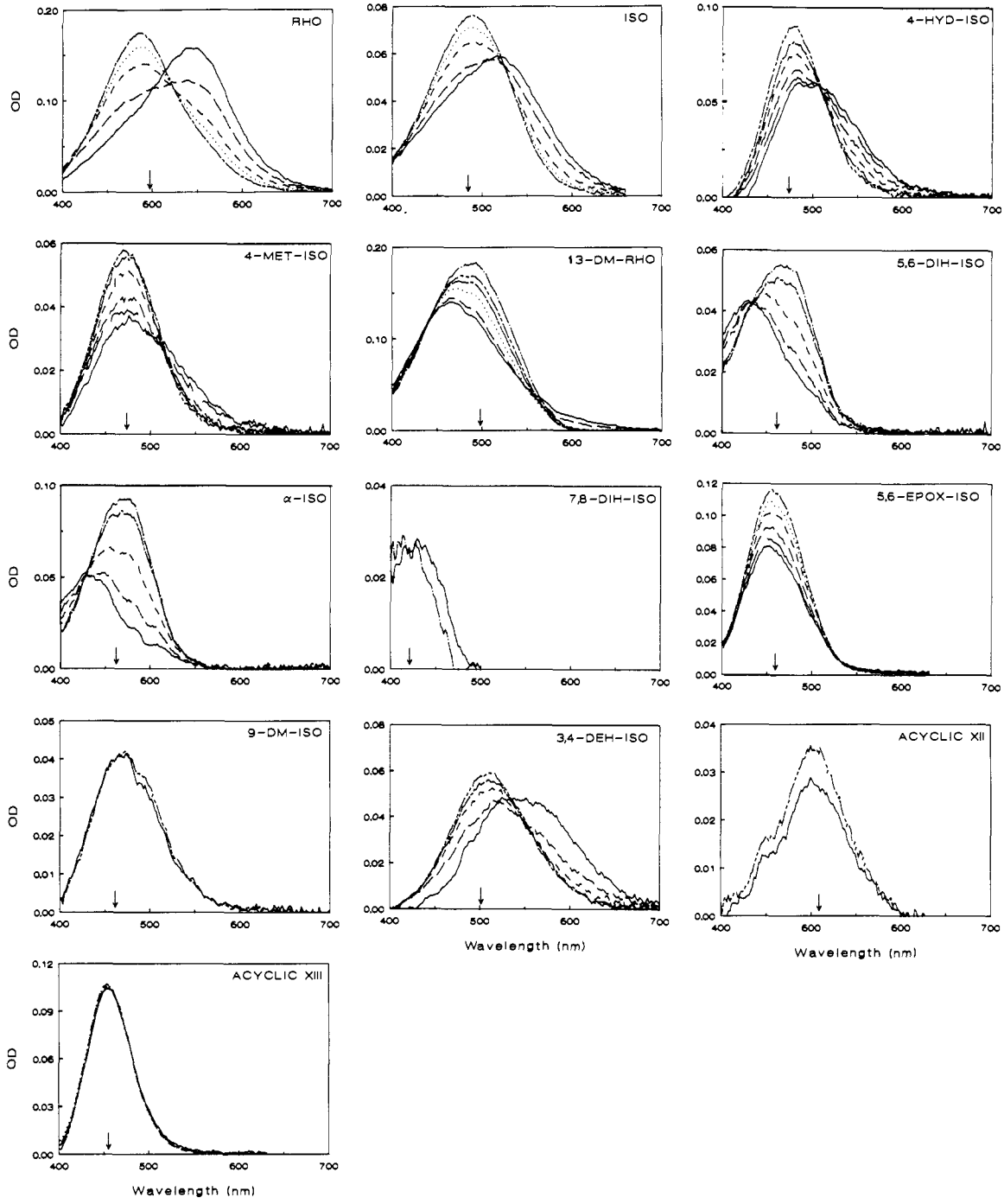


**Figure 3.** Time-dependent optical density spectra calculated by using the bleach spectra (see text). These were calculated by using either the modeled bleach compensating for back photolysis (in the case of rhodopsin), the observed bleach (the majority of the other pigments), or an estimated bleach where no measured bleach was available (iso). The arrows show the $\lambda_{max}$ of the ground-state pigment. Times after photolysis are the same as the curve styles in Figure 2.

after being bleached with one laser pulse. By modeling this bleaching spectrum we can determine the amount of pigment bleached and the spectra of any time-independent photoproducts which are formed upon photolysis. We then add back the spectrum for the correct amount of bleached parent pigment to the difference spectra and subtract the spectrum of any stable photoproducts to determine the actual absorption spectra at different times after photolysis.

In Figure 3 we present the absorption spectra corresponding to (and calculated from) the difference spectra given in Figure 2. From this analysis it is quite clear that the corrected spectra obtained after photolysis of rho, iso, the 4-substituted, and 3,4-deH-iso pigments are qualitatively similar. Each exhibits early red-shifted absorptions which decay to blue-shifted absorptions. In variance with these patterns, the other pigments exhibit early intermediate absorptions which are blue-shifted from the parent pigments or which are red-shifted but show little time evolution.

**(2) Low-Temperature Illumination Experiments.** Low-temperature (93 K) illumination experiments, followed by gradual warming up in the dark, were carried out with the previously described pigments. Figure 4 shows a low-temperature steady-state illumination experiment with 5,6-diH-iso. Illumination at 93 K with 430-nm light led to a bleaching at 470 nm and creation of a blue-shifted (BSI) photoproduct (Figure 4a). Subsequent illumination with 370-nm light caused partial regeneration of the original absorption band at 480 nm (Figure 4b). We note that the maximum (steady state) change in absorbance, obtainable for the forward (430 nm) irradiation of the pigment, is considerably larger than that of the back photoconversion with 370-nm light. This appears to be a general trend for all BSI generating pigments

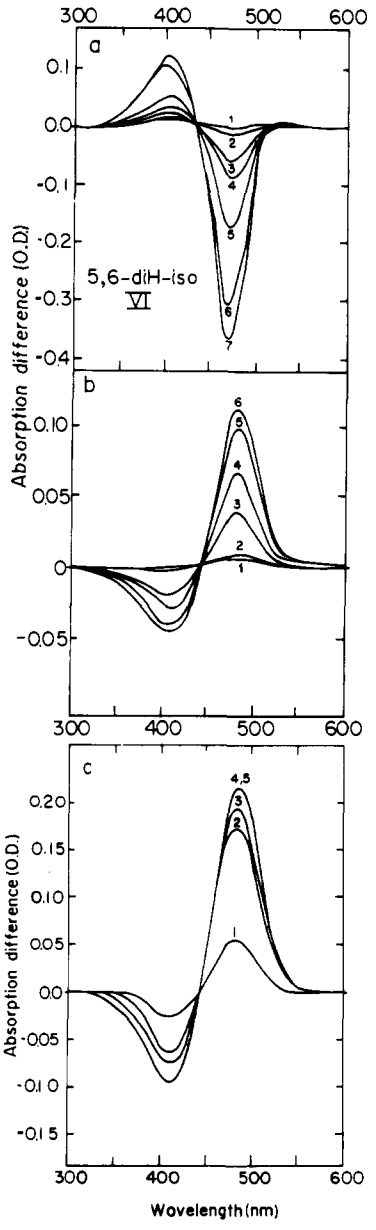


**Figure 4.** (a) Difference spectra of 5,6-diH-iso at 93 K ($\lambda_{max}$ = 461 nm, sample absorbance = 1.1) after illumination at 430 nm. Curves 1–7 represent illumination for 2, 6, 16, 46, 80, 106, and 166 s, respectively. Curve 7 represents the maximum (steady-state) absorbance change obtainable. (b) Illumination with 370-nm light of a sample which was previously illuminated with 430-nm light. Curves 1–6 represent illumination for 2, 12, 42, 102, 122, and 462 (steady-state value) s, respectively. (c) Difference spectra of 5,6-diH-iso which was irradiated first at 93 K with 430-nm light and then warmed to 113 K and subsequently to 133 K. Curve 1 is a difference spectrum between 113 and 133 K, following the warming process. Curves 2–5 are the difference spectra between 113 and the spectrum at 133 K after 5, 8, 13, and 18 min, respectively, at this temperature.

(see below) and is attributed to the relative absorbances and quantum yields at the above two wavelengths. Irradiation of a preirradiated sample with a 530-nm cutoff filter (instead of at 370 nm) did not cause any change in the absorption. This indicates that, in variance with native iso, there is no photolabile batho intermediate which absorbs to the red of 530 nm. The initially blue-shifted band which was formed following 430-nm illumination at 93 K was stable up to 130 K. Above this temperature, the difference spectrum indicated formation of a red-shifted absorption (maximum difference at 480 nm, Figure 4c) attributed to the lumi stage (see discussion below).

Similar results obtained with α-iso are shown in Figure 5. Irradiation at 93 K with 430 nm light caused significant bleaching

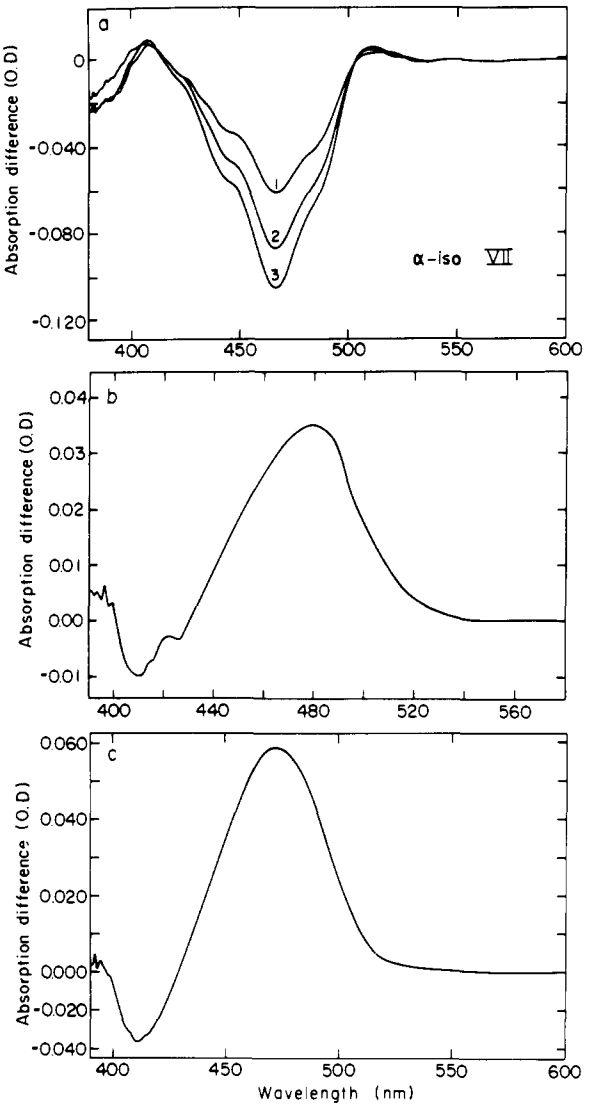


**Figure 5.** (a) Difference spectrum of α-iso at 93 K ($\lambda_{max}$ = 461 nm, sample absorbance = 0.27) after illumination with 430-nm light. Curves 1–3 represent illumination for 90, 120, and 200 (maximum, steady-state value) s. (b) Difference spectrum of α-iso after 370-nm illumination of a sample which was previously irradiated with 430-nm light for 200 s. The spectrum, recorded after 200 s, corresponds to the maximum (steady-state) value attainable with the 370-nm wavelength. (c) Difference spectrum of α-iso which was irradiated first at 93 K with 430-nm light and then warmed to 133 K. The difference spectrum is between 5 and 1 min at 133 K.

at 470 nm, accompanied by a small absorbance increase at 410 nm (Figure 5a). The presence of a blue-shifted intermediate around 410 nm was confirmed by irradiation at 370 nm, which caused partial regeneration of the 470-nm band and bleaching at 410 nm (Figure 5b). In addition, following warming of the mixture to 130 K, formation of a red-shifted absorption (480 nm) and bleaching at 400 nm was observed (Figure 5c). It should be noted that irradiation at 93 K (with 530 nm light) following pigment irradiation with 430-nm light did not cause any change in the difference spectrum. Again, this experiment indicates that there is no detectable photolabile intermediate absorbing to the red of 530 nm corresponding to a batho-like intermediate. Pigments 5,6-epox-iso (Figure 6), acyclic XII (Figure 7), and acyclic XIII and acyclic XIV (Figure 8) behave analogously to the above pigments in exhibiting a pronounced photobleaching which is not accompanied by a comparable increase in absorption in the red. Similarly, upon warming to 133 K a red shift in absorption is observed. However, all four pigments are also characterized by some contribution of a red-shifted band in the difference spectrum, following illumination at 93 K, which is photoreversible by red light.

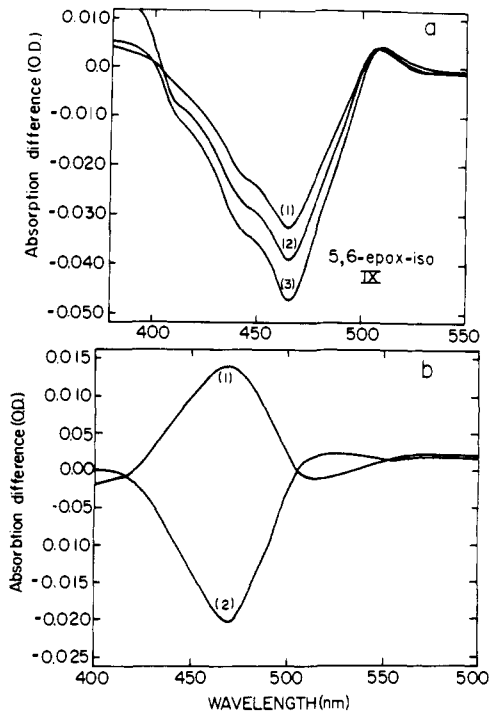


**Figure 6.** (a) Difference spectra of 5,6-epox-iso at 93 K ($\lambda_{max}$ = 465 nm, sample absorbance = 0.11) after illumination with 430-nm light. Curves 1–3 represent illumination for 80, 100, and 180 (steady-state) s, respectively. (b) (1) Difference spectrum after 200 s of 530-nm illumination of the sample obtained in (a) and (2) difference spectrum after reillumination with 480-nm light of the sample obtained in (1).

Unlike the above pigments and in keeping with its room-temperature photolysis patterns, low-temperature photolysis of 3,4-deH-iso gave results similar to those for iso. Following irradiation with 440-nm light at 93 K a bleaching was observed at 495 nm accompanied by an absorbance increase at 580 nm, corresponding to a batho intermediate. Subsequent illumination with 600-nm light reverses the effect, regenerating a band at 500 nm. Warming the mixture to 170 K (following irradiation at 600 nm) did not cause any change in the difference spectrum. The latter experiment points out that, unlike 5,6-diH-iso or α-iso, there is no detectable blue-shifted intermediate at low temperatures which initiates formation of lumi. The lumi intermediate was formed in 3,4-deH-iso upon warming to 133 K the pigment mixture which had been irradiated at 93 K with 440-nm light. Similar patterns (Figures 9 and 10) were also exhibited by 4-hyd-iso and 4-met-iso, respectively.

## Discussion

**(1) General Features.** Several major conclusions may be drawn from the respective pigment spectra and photolysis patterns shown in the previous section.

(a) The absorption spectra of visual pigments are conveniently described in terms of the "opsin-shift" which measures the energy difference between the maximum absorption of the pigment and that of a model protonated Schiff's base in methanol solution, $\lambda_{max}$ = 440 nm (for a review, including some of the presently investigated pigments, see ref 40a). As shown in Table I, all artificial pigments reported in this work exhibit opsin shifts which are close to that of native isorhodopsin (~2000 $cm^{-1}$). As previously pointed out, this implies that the basic protein–chromophore interactions which control the absorption spectrum are essentially unmodified in the artificial systems. This conclusion is now broadened, also including the $C_4$-substituted pigments. We note that the behavior in this respect differs from that of bacteriorhodopsin for which $C_4$ substitution markedly affects the opsin shift.[22] This implies that the ring-chain conformation in the $C_4$-substituted rhodopsins is similar to that of native isorhodopsin, indicating a less packed protein environment in the $C_4$ region as compared with bacteriorhodopsin.

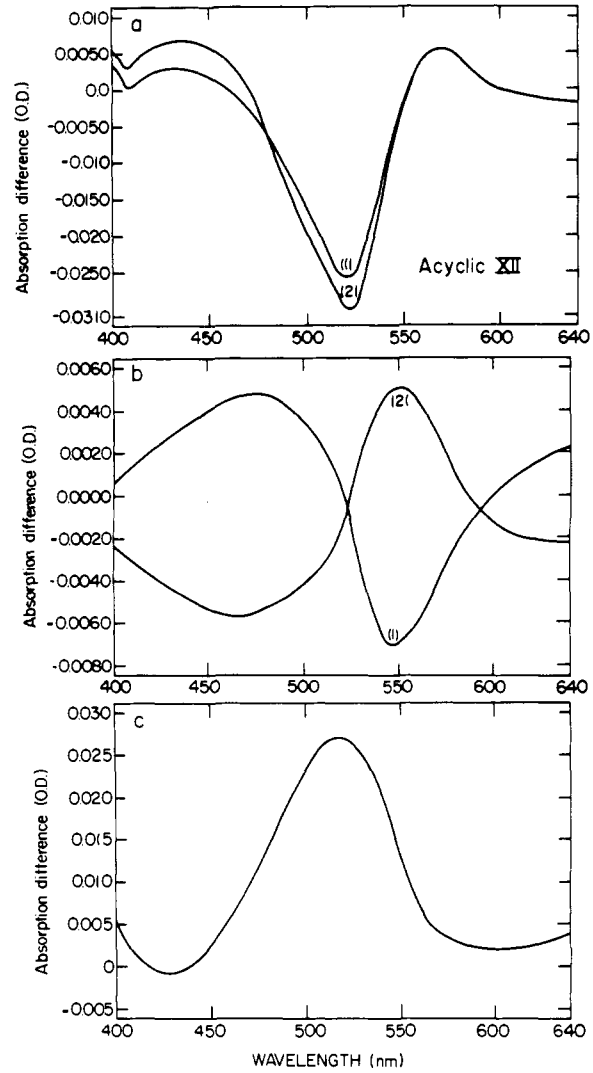


**Figure 7.** (a) Difference spectra of acyclic XII at 93 K ($\lambda_{max}$ = 505 nm, sample absorbance = 0.2) after illumination with 470-nm light. Curves 1 and 2 represent illumination for 120 and 180 (steady-state value) s, respectively. (b) (1) Difference spectrum after 200 s of 530-nm illumination of the sample obtained in (a) and (2) difference spectrum after reillumination with 470-nm light of the sample obtained in (1). (c) Difference spectrum of acyclic XII which was first irradiated at 93 K with 470-nm light and then warmed to 133 K. The difference spectrum was taken after 5 min at 133 K.

(b) For all pigments, including rho and iso, the initial change in absorbance at room temperature measured 15–20 ns after illumination cannot be described by a simple red-shifted (batho) photoproduct. In all cases, an additional blue band is present which appears only very weakly in the cases of rho, iso, and 3,4-deH-iso (see also discussion below) but markedly grows in intensity in the series: 4-hyd-iso, 4-met-iso, 13-dm-rho (or 13-dm-iso), 5,6-diH-iso, 5,6-epox-iso, and α-iso.

(c) In all of the above artificial pigments the absorption of the blue intermediate, identified as BSI, is blue-shifted with respect to the parent pigment and exhibits a lower extinction coefficient.

(d) The 9-dm-iso, acyclic XII, and acyclic XIII pigments exhibit absorbance changes which deviate in various ways from the characteristic absorbances of batho or of BSI. However, in these cases, the room-temperature absorbance changes are small and/or show little variations over a time scale of 20 ns–1 μs.

(e) The two classes of pigments, those showing a pronounced batho band at room temperature and those exhibiting a predominant BSI absorption, also behave differently at 93 K. The first exhibits the characteristic photogeneration of batho, while the latter forms the BSI intermediate. Both appear to be photoreversible to some extent (see comments below). The fact that BSI-rho has not been observed following low-temperature (93 K)

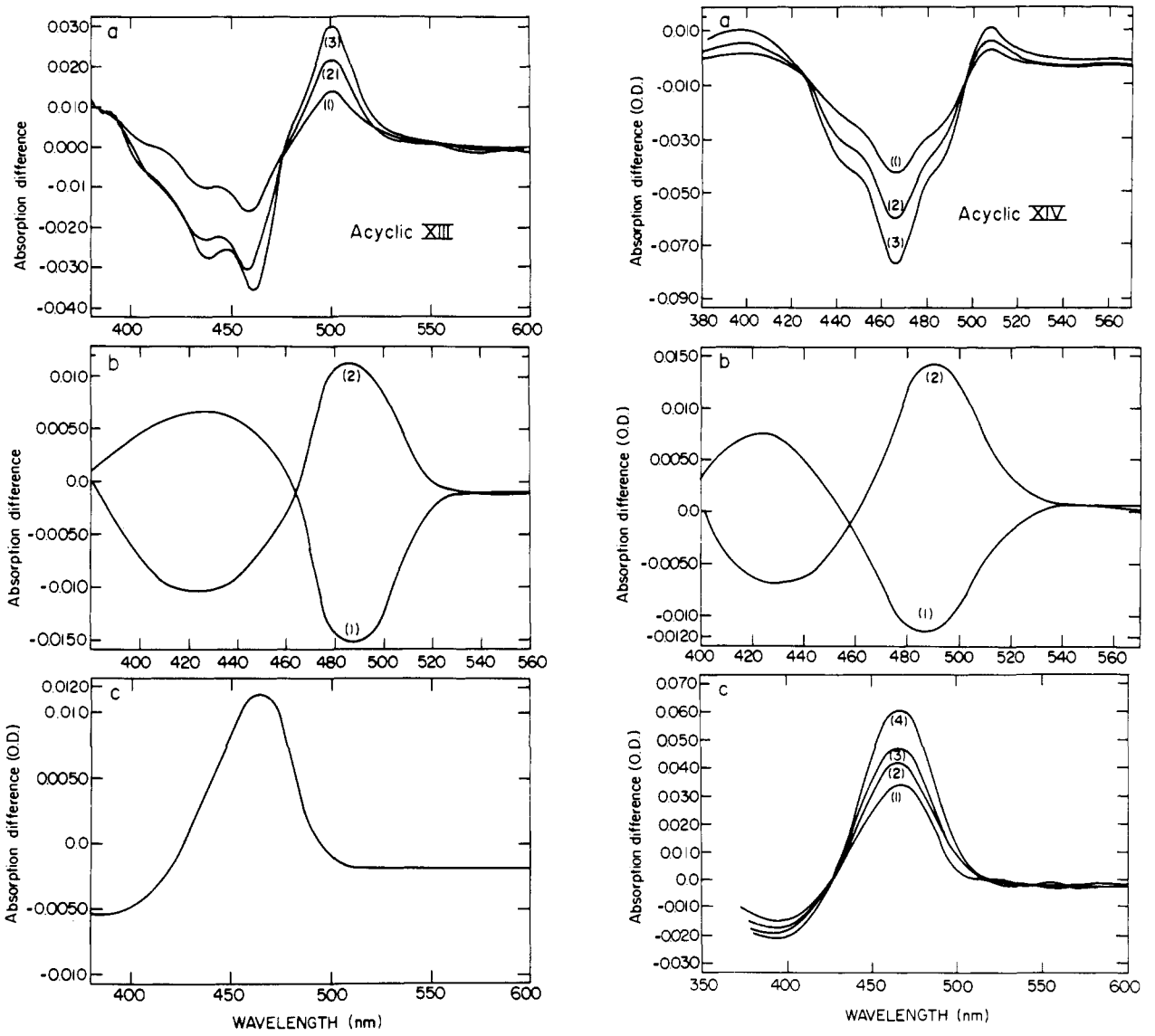


**Figure 8.** (a) Difference spectra of acyclic XIII and acyclic XIV at 93 K ($\lambda_{max}$ = 460 nm, sample absorbance = 0.15) after illumination with 470-nm light. Curves 1–3 represent illumination for 60, 120, and 180 (steady-state value) s, respectively. (b) (1) Difference spectra after 200 s of 520-nm illumination of the sample obtained in (a) and (2) difference spectra after reillumination with 430-nm light. (c) Difference spectra of acyclic XIII and acyclic XIV which were first irradiated at 93 K with 430-nm light and then warmed to 133 K. The difference spectra were taken after 10 min at 133 K.

irradiation of native rho is accounted for by the shift of the batho-rho ⇄ BSI-rho equilibrium toward batho-rho at low temperatures.[32]

With respect to the low-temperature data, we note that in some cases (pigments from IX, XII, XIII, and XIV) the formation of a red-shifted band is superimposed on the main BSI-generation patterns (Figures 6, 7, and 8). The effect, which accounts for a relatively small fraction of the primary photoreaction, is photoreversible by alternating illumination with blue and red light, without affecting the major portion of the bleached pigment and of lumi formation (see below) attributed to the BSI intermediates. At this point we should note, however, that photoreversibility is not complete. Thus, in some cases (e.g., pigments from VII, IX, XIII, and XIV), bleaching of the original pigment is associated with an apparent structure in the corresponding absorption bands (Figures 5, 6, and 8, respectively). On the other hand, subsequent illumination with either red light (pigments from IX, XIII, and XIV) or blue light (pigment from XII) regenerates an absorption band which lacks the (original) fine structure. This behavior characterizes only the primary forward and back irradiations. Thus, subsequent back and forth irradiations yield mirror spectra (Figures 6b and 8b), which are indicative of complete reversibility. We interpret these observations by assuming that the back photoreaction regenerates a pigment photostationary mixture which varies from the original pigment with respect to single bond (or double bond, see below) conformations and which lacks the fine structure in the principal absorption band. A plausible interpretation of the red light reversibility is to attribute the red-shifted photoproduct to the 11-cis isomer of the original (9-cis) pigments, in keeping with the corresponding red shifts between native rho and iso. Alternatively, the red-shifted band may represent a residual batho intermediate which does not equilibrate with BSI. In such a case the picture will be complicated by the need to involve two independent forms (binding sites) of the pigments or batho intermediates at −180 °C,[27] one yielding BSI and the second leading to batho. Work is in progress to discriminate between these two alternatives. Upon warming the 93 K illuminated pigments to 133 K, an absorbance change is observed which is red-shifted with respect to BSI. On the basis of the analogy with native rho and iso, we attribute the 133 K species as one corresponding to the lumi intermediates. However, on the basis of the present experiments, an analogous intermediate such as meta-I cannot be definitely ruled out.

**(2) Global Exponential Fitting and SVD Analysis.** The striking feature about several of the synthetic pigment analogues presented here is the presence of a blue-shifted absorption and the absence of a red-shifted absorption tens of nanoseconds after room-temperature photolysis. This is in contrast to the results for rho or

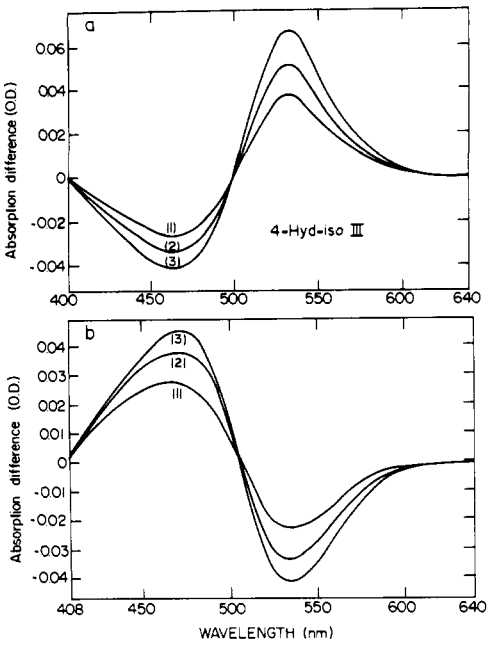


**Figure 9.** (a) Difference spectra of 4-hyd-iso at 93 K ($\lambda_{max}$ = 473 nm, sample absorbance = 0.2) after illumination with 430-nm light. Curves 1-3 represent illumination for 120, 160, and 200 (steady-state value) s, respectively. (b) (1) Difference spectra after 550-nm illumination of the sample obtained in (a). Curves 1-3 represent illumination for 120, 160, and 200 (steady-state value) s, respectively.

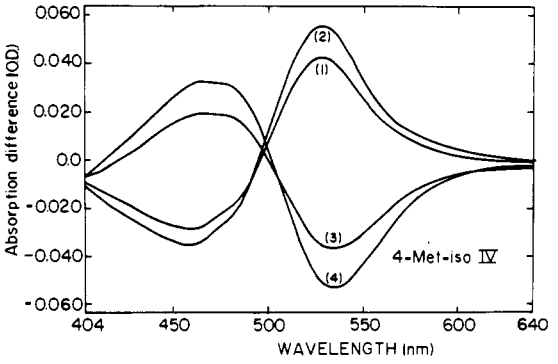


**Figure 10.** Difference spectra of 4-met-iso at 93 K ($\lambda_{max}$ = 472 nm, sample absorbance = 0.25) after illumination with 430-nm light for 120 and 160 s (curves 1 and 2). Curves 3 and 4 represent illumination with 550-nm light for 120 and 160 s, respectively, of the sample irradiated previously with 430-nm light.

iso, where batho is the predominant transient species at this time. Since a blue-shifted intermediate consistently presented itself after photolysis of the artificial pigments we studied, we conjectured that the same intermediate might be present in rho. Improved methods of analysis (global exponential fitting and SVD) of photolysis data from rho led to the conclusion that Scheme I, which proposes the existence of a blue-shifted absorber on what is traditionally accepted as the batho time scale, did indeed explain our data.[32]

Keeping Scheme I in mind, it is now possible to reconcile the results from the pigments reported here with the results from rho. We discuss here the results of analyses of rho, iso, 13-dm-rho, 5,6-diH-iso, α-iso, 3,4-deH-iso, 4-hyd-iso, and 4-met-iso for which high signal-to-noise data is available. By using the SVD/global exponential fitting procedure, we are able to simultaneously analyze absorption measurements at all wavelengths and times. From this analysis it is possible to deduce the number of processes occurring during the observation period, the apparent (or observed) rate constants of these processes, and the corresponding preexponential factors (referred to as the "b-spectra"). Once a mechanism has been proposed, it is often possible to calculate the

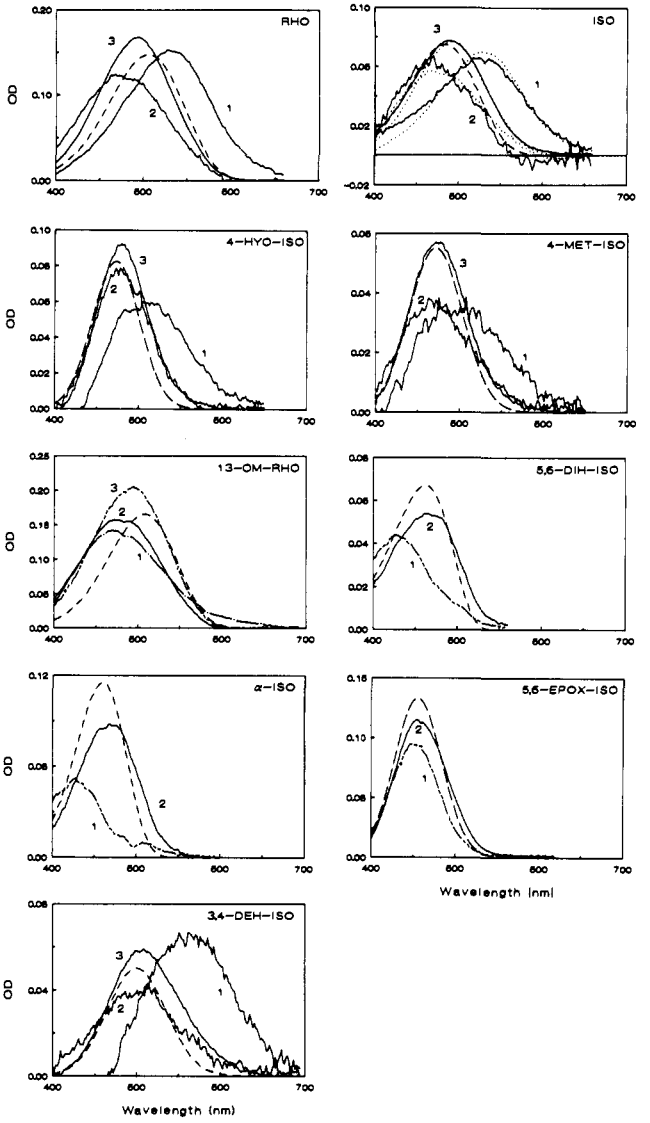


**Figure 11.** Spectra of the intermediates. The spectra of the intermediates are shown for each pigment with numbers to denote the order of appearance. Generally curve 1 corresponds to the batho spectrum, curve 2 to the BSI spectrum, and curve 3 to the lumi spectrum. The dashed line (---) shows the bleaching spectrum of ground-state pigment. In the iso figure the corresponding rho intermediates are shown with dotted lines for comparison. In the 13-dm-rho, 5,6-diH-iso, 5,6-epox-iso, and the α-iso figures, the first intermediate is presumably the equilibrated mixture of batho and BSI and the second spectrum is that of lumi. In the case of iso the intermediates were calculated assuming an equilibrium constant equal to that found for rho (1.4). In the case of 3,4-deH-iso, a higher equilibrium constant was required to eliminate the negative optical density observed for BSI in the red portion of the spectrum. Here the value 3.0 was used. Similarly for 4-hyd-iso and 4-met-iso values of 2.0 and 10, respectively, were used.

actual rate constants and absorption spectra of the intermediates by using the above information.

As reported previously[32] and noted above, by using this method of analysis we showed that the difference spectra measured after photolysis of rho were consistent with a mechanism involving two apparent rate constants corresponding to lifetimes at 20 °C of 36 and 215 ns. The simplest mechanism which was consistent with all of our measurements on rho (which included different photolysis wavelengths, laser pulse energies, temperatures, and measurements of transition polarizations) was Scheme I. The spectra of each of the intermediates on this time scale, batho-rho ($\lambda_{max}$ = 529 nm), BSI-rho ($\lambda_{max}$ = 477 nm), and lumi-rho ($\lambda_{max}$ = 490 nm) are presented in Figure 11. We also concluded that in rho the room-temperature equilibrium constant for the batho-rho ⇄ BSI-rho equilibrium is about 1.4, with a lifetime of

the forward reaction batho-rho → BSI-rho ($1/k_{12}$) equal to about 75 ns, and the lifetime of the back reaction BSI-rho → batho-rho ($1/k_{21}$) equal to about 110 ns at room temperature.[32] Because the time constants of formation and decay of the batho-rho ⇄ BSI-rho mixture ($1/k_{23}$) are comparable, lumi-rho is formed before the equilibrium is established.

When the data from iso photolysis are globally analyzed it is found that two processes are occurring here too, with observed lifetimes of 37 and 186 ns. Although there are a number of mechanisms which could be proposed to fit these rate constants, it seems reasonable to test whether the same basic mechanism found for rho holds for the photolysis of this pigment. Thus, we determined the actual spectra of intermediates for iso by assuming that Scheme I was appropriate. Because we had measured the difference spectra after photolysis of rho at several temperatures, we were able to calculate the batho-rho ⇄ BSI-rho equilibrium constant. In the absence of the temperature dependence for iso spectra we used the same equilibrium constant for iso as was calculated for rho at room temperature (1.4) in order to calculate the spectra of the intermediates. These spectra, for batho-iso ($\lambda_{max}$ = 530 nm), BSI-iso ($\lambda_{max}$ = 475 nm), and lumi-iso ($\lambda_{max}$ = 488 nm) are also presented in Figure 11. There is a striking similarity between the iso photolysis intermediates and those of rho (for ease of comparison the spectra of the rho intermediates are shown by dotted lines in the iso portion of Figure 11). Had we used a different equilibrium constant to calculate these spectra, significant differences may well have appeared between the photoproducts of rho and of iso. However, in the absence of an actual measurement of the batho-iso ⇄ BSI-iso equilibrium constant, it seems reasonable to note that the spectral similarities between the photoproducts of rho and iso would be a remarkable coincidence were this *not* the correct equilibrium constant. We thus conclude that not only does the photolysis of iso lead to the same basic thermal decay mechanism as the photolysis of rho but also that on this time scale the photointermediates formed after photolysis of rho are the same within our experimental error as those formed after photolysis of iso. Thus it is clear that isomerization has occurred at the batho stage since both rho and iso form batho's which have the same behavior, and only an all-trans chromophore could be reached in a single step from both these cis isomers.

When the global exponential fitting routine and SVD were used to analyze the difference spectra acquired after photolysis of 13-dm-rho, it was found (see Figure 11) that the early spectrum could be modeled as the sum of two log-normal components, with an 80% contribution from an absorber with $\lambda_{max}$ = 470 nm (BSI-13-dm-rho) and a 20% contribution from an absorber with $\lambda_{max}$ = 530 nm (batho-13-dm-rho).[29] These wavelengths correspond well to those of BSI-rho (477 nm) and batho-rho (529 nm). We thus proposed that in 13-dm-rho a batho BSI steady state has been reached faster than the ~10 ns resolution of the pulsed photolysis apparatus. This mixture then decays to lumi-13-dm-rho ($\lambda_{max}$ = 480 nm) with a lifetime of 100 ns, which then decays to meta-I-13-dm-rho ($\lambda_{max}$ = 490 nm) with a lifetime of 1200 ns. This interpretation suggests that removal of the 13-methyl group significantly alters the rate at which some of the dark reactions occur after photolysis but does not significantly alter the absorption spectra of the individual intermediates.

An analogous situation prevails in the case of 5,6-diH-iso where the discovery of a blue-shifted intermediate on the batho time scale first led us to identify the BSI species.[30] In Figure 11 we now present results of a global exponential fit and SVD analysis applied to the 5,6-diH-iso data. Interestingly, while the maximum of the spectrum from the first intermediate is blue-shifted from the parent pigment, it also has a broad tail to the red of the parent pigment. Although an increase in OD to the red of the parent pigment in 5,6-diH-iso is apparent in the 20 ns difference spectrum shown in Figure 2, we originally had attributed this to the growing-in of the lumi intermediate.[28] Were this entirely true, our present SVD analysis would not have resulted in a broad red tail on the first intermediate. It thus appears that the photoproducts created after photolysis of 5,6-diH-iso are also consistent with our proposed mechanism for rho photolysis. That is, the first spectrum would represent the batho-5,6-diH-iso/BSI-5,6-diH-iso mixture which equilibrated on a time scale faster than our time resolution, and where the equilibrium, as for 13-dm-rho, is shifted largely toward BSI. The second spectrum, lying nearer to that of the parent pigment, would represent lumi-5,6-diH-iso. From these spectra we estimate that the absorption maxima of the intermediates are about 430 nm for BSI-5,6-diH-iso, 470 nm for lumi-5,6-diH-iso, and 510 nm for batho-5,6-diH-iso. The lifetime for decay of the first intermediate spectrum (the batho ⇄ BSI mixture) to the second spectrum (lumi) is 182 ns.

In the global analysis for α-iso, as for 5,6-diH-iso, it was found that a single exponential was adequate to fit the data, with a rate constant coresponding to a lifetime of 165 ns, very close to that of 5,6-diH-iso. Also similar to the results of 5,6-diH-iso, the first intermediate appears to be the sum of two components, one of which is blue-shifted (428 nm) from the parent pigment (461 nm) and the other of which is red-shifted (to about 515 nm). The second intermediate lies slightly to the red of the parent pigment at 470 nm. Thus, the results from this pigment are also consistent with Scheme I. We propose that, like in 5,6-diH-iso, the first intermediate which we observe after photolysis of α-iso is actually a mixture of batho-α-iso and BSI-α-iso, compromised mainly of the BSI component. This mixture then decays with a lifetime of 165 ns to lumi-α-iso. Similar results were obtained from 5,6-epox-iso photolysis. Again a predominantly BSI photoproduct was observed immediately following photolysis which decayed to lumi-5,6-epox-iso with a lifetime of 149 ns.

A distinct contrast to the above results is found in the analysis of the 3,4-deH-iso data. For this pigment we obtain lifetimes of 24 and 148 ns; the first corresponding to the decay of batho to BSI and the second to the decay of the batho ⇄ BSI equilibrium mixture. In performing a global analysis to obtain the intermediate spectra, a larger equilibrium constant value was required in order to prevent significant negative optical density for the BSI intermediate. The same problem, to a less pronounced degree, was observed for the iso data shown in Figure 11, but the negative optical density for BSI in that case was considered to be within experimental error. An equilibrium constant of 2.0 removed the negative optical density for the BSI-iso spectrum (resulting in even better agreement with the intermediate spectra from rho photolysis than is shown in Figure 11), and it is possible that both of these 9-cis pigments have somewhat larger equilibrium constants than is observed for rho photolysis. Temperature dependence studies will be required to validate this assumption.

Similar behavior was observed for the two 4-substituted pigments. In both, decay of an initial batho product to an equilibrated batho-BSI mixture was resolved followed by subsequent decay to lumi. For 4-hyd-iso the lifetimes were 49 and 401 ns, and for 4-met-iso they were 25 and 124 ns. Again, higher equilibrium constants were required (2.0 for 4-hyd-iso and ~10 for 4-met-iso) to eliminate negative ODs from the BSI intermediate spectra. While we were not able to perform more quantitative analysis for the 7,8-diH-iso pigment, it seems to be more similar to the 5,6-diH-iso or α-iso pigments (in that, if a red-shifted absorber is present at early times after photolysis on our time scale, the amount is small). Quantitative analyses of acyclic XII, acyclic XIII, and 9-dm-iso were also not possible; these pigments showed little evolution of their intermediate spectra on the 10 ns–1 μs time scale.

**(3) BSI Formation and Decay Kinetics.** The new intermediates appearing between the batho and lumi stages have similar spectra in all of the pigments studied, and these spectra lie somewhat to the blue of the lumi spectrum of each of the pigments. In some pigments the back reaction from BSI to batho has a rate similar to the decay of BSI to lumi. In native rhodopsin the BSI intermediate has an enthalpy 3 kcal above that of batho. Thus, while the batho ⇄ BSI equilibrium constant at room temperature is ~1.4 in rho, it becomes much smaller at low temperatures. Previous studies of rho photolysis intermediates performed at low temperatures have not detected BSI since at temperatures at which batho is stable the BSI batho equilibrium constant is on the order of $10^{-3}$.

**Table I.** Absorption Maxima and Lifetimes for Intermediates After Photolysis of Rho and Several Visual Pigment Analogues

| | absorption maximum (nm) | | | | | lifetime (ns) | | | |
|---|---|---|---|---|---|---|---|---|---|
| absorber | PSB[a] | parent | batho | BSI | lumi | slow[b] | fast[c] | $K_{eq}$ | opsin shift ($cm^{-1}$) |
| rho (I) | 440 | 498 | 529 | 477 | 490 | 215 | 36 | 1.4 | 2650 |
| iso (II) | 440 | 483 | 530 | 475 | 488 | 186 | 37 | 1.4 | 2000 |
| 4-hyd-iso (III) | 426 | 473[d] | 506 | 477 | 479 | 401 | 49 | 2.0 | 2300 |
| 4-met-iso (IV) | 426 | 472[d] | 490 | 465 | 475 | 124 | 25 | >5 | 2300 |
| 13-dm-rho (V) | | 495 | 530[e] | 470[e] | 480 | 100 | | >5 | |
| 5,6-diH-iso (VI) | 422 | 461[f] | 510[e] | 430 | 470 | 182 | | >5 | 2000 |
| α-iso (VII) | 422 | 461[f] | 515[e] | 428 | 470 | 165 | | >5 | 2000 |
| 7,8-diH-iso (VIII) | 392 | 421[f] | | ~420[g] | 415[h] | *i* | | | 1800 |
| 5,6-epox-iso (IX) | 416 | 459[d] | 490 | 440 | 460 | 149 | | >5 | 2250 |
| 9-dm-iso (X) | 422 | 461[f] | | | | *i* | | | 2000 |
| 3,4-deH-iso (XI) | 450 | 500[f] | 560 | 500 | 505 | 148 | 24 | 3.0 | 2200 |
| acyclic XII | 462 | 505[f] | | | | *i* | | | 1850 |
| acyclic XIII | 420 | 460[f] | | | | *i* | | | 2100 |
| acyclic XIV | 420 | 460[f] | | | | | | | 2100 |

[a] Protonated Schiff's base values are from methanol solution. [b] These lifetimes correspond to the second observed lifetime for those pigments where two lifetimes were needed to fit the data, except for 13-dm-rho, where it corresponds to the first observed lifetime. This represents the lifetime for the decay of the batho/BSI mixture. [c] These lifetimes correspond to the observed lifetime of batho decaying toward equilibrium with BSI. [d] This work. [e] Estimated by decomposing the first intermediate spectrum obtained from the SVD analysis into two components. [f] These pigments were measured previously. See ref 40a for a review. [g] Estimated from the absorption spectrum measured 20 ns after photolysis. We attribute this to BSI since the red shift from the parent pigment is much smaller than for the other pigments where batho is evident. However, it is also possible that this spectrum actually represents a mixture of the batho and BSI components. [h] Estimated from the absorption spectrum measured 4000 ns after photolysis. [i] Not enough data available to determine the lifetime.

While spectra of the BSI intermediates in the artificial pigments studied here are quite similar, the kinetics of the formation of BSI and the approach to equilibrium change dramatically with different retinal modifications. Artificial pigments investigated here primarily include those with retinals having disrupted or extended ring conjugation, $C_4$-substituted retinals, retinals whose rings have been replaced with short chain segments, and demethylated retinals. Most of these modifications result in acceleration of the batho to BSI transition, some dramatically so, relative to the kinetics found in native rho. The back reactions from BSI to batho tend to be accelerated to a lesser extent if at all. This results in a more pronounced spectral contribution from BSI relative to that of batho on a 10-ns time scale after photolysis. The rates for these processes vary with retinal modification, resulting in different equilibrium concentrations of batho and BSI. However, the observed behaviors of all the pigments studied here can be rationalized by Scheme I.

It is now well accepted that the stage of bathorhodopsin represents an isomerized all-trans chromophore.[2,3,5,8,10,43,44] However, the resonance Raman spectrum of bathorhodopsin shows unusually intense hydrogen out-of-plane wagging vibrations in the 800–920-$cm^{-1}$ region, which indicate that the chromophore is conformationally distorted.[20,43,44] FTIR data indicate that the transition from batho to lumi involves a relaxation of the above strain via conformational changes both in the retinal chromophore and in the protein.[20,45,46] We suggest that modification of the polyene affects the retinal–protein interactions at the batho stage. Consequently, the initially formed batho is destabilized and undergoes a fast change in the retinal conformation which results in the BSI intermediate. Such a strain relief in BSI is indeed supported by FTIR studies with 5,6-diH-iso and 13-dm-iso.[47] In native rho, generation of the BSI intermediate is slower either because this retinal conformation change is blocked or occurs simultaneously with slower protein conformational changes.

While the kinetics of BSI formation are strongly affected by a variety of chromophore structural changes, the BSI-to-lumi decay kinetics are very similar. These rates are even more similar than the slow lifetime values contained in Table I show. In the case of the three largest values there, significant back reaction from BSI to batho prolongs the observed lifetime reported there relative to the actual lifetime (reciprocal of the forward rate). The similarity of BSI decay rates suggests that the BSI formation kinetics are controlled by chromophore–protein interactions, while the decay kinetics are primarily determined by protein changes. It is interesting that chromophore changes both at the ionylidene ring and along the polyene chain strongly affect BSI formation kinetics. This suggests that the barrier to BSI formation is affected by steric interactions between the chromophore and protein at a number of points along the polyene chain.

Interactions at the ring are clearly important as even subtle changes such as removal of ring conjugation greatly accelerate the kinetics. This suggests that isomerization resulting in batho formation leaves the chromophore in a strained state and that relief of this strain as BSI forms requires movement of the ring to overcome some protein steric barrier. Removing ring conjugation makes the ring–polyene orientation more flexible and accelerates BSI formation. This can also be seen in the $C_4$-substituted pigments. Small substituents at $C_4$ lead to pigments which behave like native rhodopsin. As the substituent gets larger the BSI formation kinetics accelerate, and the equilibrium between batho and BSI increasingly favors BSI.

While ring–protein interactions are clearly important, chain substituents are also important for BSI formation kinetics. Removal of the 13-methyl group, for instance, shifts the batho–BSI equilibrium, though not as strongly as ring alterations. Again, it is likely that removal of the strain in the chromophore at the batho stage involves chromophore motions which bring the 13 methyl group into contact with the protein. Interactions of the 9-methyl group are also clearly important, but it is not yet as clear how individual rates are affected by removal of this methyl group.

**(4) Spectra and Energy Storage in Intermediates.** In most of the pigments the room-temperature spectrum of BSI is blue-shifted with respect to the parent rhodopsin and is also characterized by a reduced oscillator strength. Independent of the exact values of $\lambda_{max}$ and oscillator strength, the question arises as to the mechanism accounting for the spectrum of BSI. No definite suggestion can be made at this time, since at present even the spectra of rhodopsin and isorhodopsin, and especially the basic red shift in batho, are not fully understood. Several factors, such as external protein charges,[15,40,21] Schiff's base counter ion and H-bond interactions,[34a,49,50] and single bond rotations,[51] may

(43) Eyring, G.; Curry, B.; Mathies, R.; Palings, I.; Lugtenburg, J. *Biochemistry* **1980**, *19*, 2410–2418.
(44) Eyring, G.; Curry, B.; Broek, A.; Lugtenburg, J.; Mathies, R. *Biochemistry* **1980**, *21*, 384–393.
(45) Rothschild, K. J.; DeGrip, W. J. *Photochem. Photobiophys.* **1986**, *13*, 245–258.
(46) DeGrip, W. J.; Gillespie, J.; Bovee-Gwerts, P. H. M.; Rothschild, K. J. In *Retinal Proteins*; VNU Science Press: Utrecht, **1987**; pp 133–143.
(47) Ganter, U. M.; Gartner, W.; Siebert, F. *Eur. Biophys. J.* **1990**, *18*, 295–299. Ganter, U.; Kashima, T.; Sheves, M.; Siebert, F., submitted to *J. Am. Chem. Soc.*
(48) Sheves, M.; Friedman, N.; Albeck, A.; Ottolenghi, M. *Biochemistry* **1985**, *24*, 1260–1265.

participate in determining the spectrum of the chromophore. It is plausible that a change in distance between the polyene and a protein negative charge which causes the red shift in batho is reversed upon forming BSI. Consistent with this idea are linear dichroism measurements[52] showing that both rho → batho and batho → BSI transitions are associated with major changes in the orientation of the polyene chromophore.

Given its blue-shift, it is interesting that the BSI intermediate lies 3 kcal/mol above the batho intermediate. This calls into question earlier suggestions[6,7,16,18] that the red shift and energy storage are essentially associated with the same mechanism. One might then ask at what stage after formation of the primary photoproduct the energy stored in chromophore–protein interactions is transferred to the protein. One possibility is that energy storage is not associated at all with the chromophore, namely that energy has been channeled into the protein as early as the stage of batho or even photo. Alternatively, energy stored in the chromophore at the batho stage may be transmitted to the protein as batho is converted to BSI. This is consistent with the disappearance of chromophore HOOP modes detected by FTIR and with the blue-shifted absorption of BSI. This may be due to relief of strain in the chromophore. Presumably the relaxation of this strain in BSI would lead to reduction of the large, negative circular dichroism of batho[53] (potentially measurable in the case of the pigments where BSI forms at low temperatures) in keeping with the FTIR data of Gartner et al.[47] Such a model could also provide the moving force for the protein change required to move to the lumi stage. This could be provided directly by the contacts which store the strain energy in BSI. Alternatively, it could result from protein movement into void space potentially opened by distortion of BSI along one wall of the pocket. Either of these mechanisms could plausibly trigger protein change prevented by the presence of the better fitting cis chromophores.

Finally, the fact that the batho ⇄ BSI equilibrium favors BSI is particularly interesting in light of the fact that there is a 3 kcal positive enthalpy difference between these two states. This dictates that this reaction be entropically driven. This situation could arise from protein changes at the BSI stage, but protein changes need not be invoked. Many lines of evidence show that the chromophore is in a twisted strained conformation at the batho stage, and plausibly it is in a more relaxed conformation at the BSI stage. This would give it more degrees of freedom in BSI thus making BSI a higher entropy state. Synthetic chromophore structural changes might then affect the batho enthalpy relative to the transition state and BSI so that the rate of batho to BSI would be accelerated while the back reaction would be less affected. Further work is needed to test these possibilities for spectral and kinetic properties of these intermediates.

**Acknowledgment.** The authors thank Prof. R. S. H. Liu for the gift of 11-*cis*- and 9-*cis*-13-desmethylretinals. This research was supported by a grant from the Eye Institute of the National Institutes of Health (EY 00983) and by the U.S.-Israel Binational Science Foundation and by the fund for basic research (administered by the Israel Academy of Sciences and Humanities).

(49) Baasov, T.; Friedman, N.; Sheves, M. *Biochemistry* **1987**, *26*, 3210-3217.
(50) Lugtenburg, J.; Muradin-Szwezkowska, M.; Heeremans, C.; Pardoen, J. A. *J. Am. Chem. Soc.* **1986**, *108*, 3104-3105.
(51) Shichida, Y.; Kropf, A.; Yoshizawa, T. *Biochemistry* **1981**, *20*, 1962-1968.
(52) Lewis, J. W.; Einterz, C. M.; Hug, S. J.; Kliger, D. S. *Biophys. J.* **1989**, *56*, 1101-1111.
(53) Yoshizawa, T.; Shichida, Y. *Methods Enzymol.* **1982**, *81*, 634-641.

# Intramolecular [2 + 2] Photocycloaddition. 10.[1] Conformationally Stable *syn*-[2.2]Metacyclophanes

**Jun Nishimura,* Yoichiro Horikoshi, Yasuhiro Wada, Hideo Takahashi, and Mitsuo Sato**

*Contribution from the Department of Chemistry, Faculty of Engineering, Gunma University, Tenjin-cho, Kiryu 376, Japan.* *Received September 20, 1990*

**Abstract:** Three isomerized 1,2:9,10-diethano-*syn*-[2.2]metacyclophanes **5**, **6**, and **7** were prepared from *cis*-1,2-bis(*m*-vinylphenyl)cyclobutane by photocycloaddition. Their yields were 10, 5, and 3%, respectively. $^1$H NMR chemical shifts of aromatic protons for cyclophane **5** clearly suggest the syn conformation. It has a rigid structure, according to its VT NMR spectra. The structure was thoroughly analyzed by X-ray crystallography. It became clear that the aromatic nuclei of this syn conformer are not arranged parallel but tilted by ca. 31-34° toward each other. Since the MM2 calculation for parent *syn*-[2.2]metacyclophane (**1**), as well as compounds **5**, **6**, and **7**, gives the tilted structure, the cyclobutane ring systems are not responsible for tilting. Therefore, these cyclobutane-fused compounds are concluded to be good models for *syn*-[2.2]-metacyclophane (**1**), whose structure has not been fully explored in detail yet. Cyclophanes **6** and **7** are also concluded to have syn conformation. Their structures were determined by NMR experiments and UV spectroscopy. Their conformations are stable in a solid state, yet in a solution (in $CDCl_3$, benzene, etc.) they slowly interconverted to each other. The initial rates were $0.29 \times 10^{-6}$ and $0.44 \times 10^{-6}$ s$^{-1}$ at 20 °C for **6** and **7**, respectively. At 20 °C, the isomer ratio of **6** to **7** was 60:40 at equilibrium. The conformational change should occur through an unstable, probably short-lived anti conformer that could not have been detected yet. The mechanisms for the interconversion and also for the photocycloaddition are proposed.

*syn*-[2.2]Metacyclophane (**1**), being unknown for a long time, was finally prepared by Mitchell and his co-workers,[2] using a chromium tricarbonyl complex in the ring-contraction step. The compound was reported to be conformationally stable at low temperatures but to change its conformation to a more stable anti one at higher than 0 °C. Its X-ray crystallographic analysis has not been achieved yet. Naturally, it is not denied that it would be possible at a reduced temperature. Fusing cyclobutane rings at the tethers seems to be one of the ways to make this syn

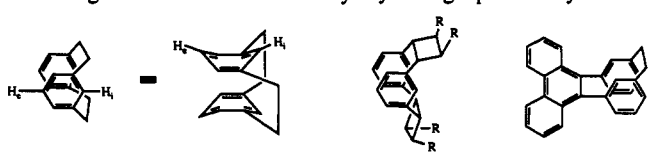


1 2 3

R=Ph, Napht, COOMe

(1) Part 9: Nishimura, J.; Takeuchi, M.; Takahashi, H.; Sato, M. *Tetrahedron Lett.* **1990**, *31*, 2911.
(2) (a) Mitchell, R. H.; Vinod, T. K.; Bushnell, G. W. *J. Am. Chem. Soc.* **1985**, *107*, 3340. (b) Mitchell, R. H.; Vinod, T. K.; Bodwell, G. J.; Weerawarna, K. S.; Anker, W.; Williams, R. V.; Bushnell, G. W. *Pure Appl. Chem.* **1986**, *58*, 15. (c) Mitchell, R. H.; Vinod, T. K.; Bushnell, G. W. *J. Am. Chem. Soc.* **1990**, *112*, 3487.

0002-7863/91/1513-3485$02.50/0 